sustainability

MDPI

Article

Biosorption of Cd(II), Co(II), and Cu(II) onto Microalgae under Acidic and Neutral Conditions

Jesse T. Phiri and Sanghwa Oh *

School of Architectural, Civil, Environmental and Energy Engineering, Kyungpook National University, Daegu 41566, Republic of Korea; jesset.phiri@knu.ac.kr
* Correspondence: shoh@knu.ac.kr; Tel.: +82-53-950-5609

Abstract: The biosorption of Cd, Co, and Cu onto three microalgae species (*Chlorella vulgaris*, *Scenedesmus* sp., and *Spirulina platensis*) was compared to determine the microalgae's capability for heavy metal adsorption in acidic and neutral environments. The Langmuir, Freundlich, and Dubinin–Radushkevich isotherm models were used to characterize the adsorption of the heavy metals onto microalgae. The maximum adsorption capacity (q_{max}) determined using the Langmuir and D-R model showed results in the order of Cu > Co > Cd in both acidic and neutral conditions. A shift from acidic to neutral conditions increased the microalgae's adsorption affinity for heavy metals, as determined using the Freundlich parameter (K_F). The adsorption affinity of the biomass for Cd and Co was in the order *S. platensis* > *C. vulgaris* > *Scenedesmus* sp. while that of Cu was in the order *C. vulgaris* > *Scenedesmus* sp. > *S. platensis*. In addition, it was found that the adsorption of Cd and Co enhanced the production of Dissolved Organic Content (DOC) as a byproduct of biosorption, whereas the adsorption of Cu appeared to suppress the generation of DOC. The mean adsorption energy (*E*) values computed by the D-R model were less than 8 (kJ/mol), indicating that physisorption was the primary force of sorption in both acidic and neutral settings. The findings of this study suggest that microalgae may be used as a low-cost adsorbent for metal removal from industrial effluent.

Keywords: biosorption; heavy metals; microalgae; adsorption models; acidic environment; neutral environment

Citation: Phiri, J.T.; Oh, S. Biosorption of Cd(II), Co(II), and Cu(II) onto Microalgae under Acidic and Neutral Conditions. *Sustainability* **2024**, *16*, 6342. https://doi.org/10.3390/su16156342

Academic Editor: Francesco Ferella

Received: 24 May 2024
Revised: 14 July 2024
Accepted: 17 July 2024
Published: 24 July 2024

1. Introduction

Heavy metals are elements with high atomic weights and densities that are at least five times greater than that of water [1]. They are naturally present in soils in small amounts; however, their excessive accumulation can degrade soil quality and harm surface plants [2]. Due to the increasing awareness of the detrimental impacts of global warming on the environment, there has been a global initiative to implement significant reforms in the transportation and energy sectors. Over the past decade, the worldwide proportion of new passenger electric vehicles (EVs) has surged, growing by approximately 50% annually [3]. Furthermore, the energy sector has undergone substantial transformations, marked by the expansion of solar and wind energy plants [4,5], both reliant on batteries for efficient energy storage. Consequently, there has been a heightened demand for Cadmium (Cd), Cobalt (Co), and Copper (Cu) to manufacture EV batteries, as well as storage systems for solar and wind energy. Cd finds widespread use in rechargeable batteries [6,7], particularly in Nickel-Cadmium (Ni-Cd) batteries, commonly employed in accessories like phones, laptops, and other durable devices. Co is a key component in the production of EV batteries [8,9], while Cu is commonly utilized in the construction of wires for current circulation in both EVs and power plants [10]. The rising demand for these metals has resulted in their accumulation in wastewater. The adverse effects of heavy metals encompass water source contamination, toxicity to aquatic life, and bioaccumulation in the food chain, which pose significant health risks to humans and wildlife [2,11].

Significantly, these metal deposits are often concentrated in economically developing nations [12], including the Democratic Republic of the Congo (DRC), Peru, Zambia, and Indonesia. Undertaking the removal of metal ions from mine effluents poses an economic challenge for these countries, given the limitations of conventional methods such as reverse osmosis, electro-dialysis, solvent extraction, and the like. Consequently, the extraction of these minerals frequently results in the inadequate treatment of mine effluents, leading to their improper disposal and eventual contamination of surface waters [13–17]. The consumption of water contaminated with heavy metals has been associated with various diseases, including Sclerosis, Alzheimer's, muscular dystrophy, and cardiovascular diseases [18]. To mitigate the occurrence of such illnesses, it is crucial to explore cost-effective metal removal techniques that can be easily implemented on a small scale by members of local communities facing water pollution issues due to mining activities.

Adsorption is the process of removing molecules or ions from a gas or liquid by binding them to the surface of another substance. The attached molecule or ion is referred to as the adsorbate, while the surface to which they adhere is the adsorbent. Adsorption serves as a cost-effective alternative to traditional methods of metal removal from wastewater, given the versatility of potential adsorbents spanning from materials such as corncob, coffee beans, rice husks, stone powders, and even microorganisms like microalgae [19–22]. Compared to traditional physiochemical methods of heavy metal removal, microbial remediation is recognized as an effective and eco-friendly approach. It offers several advantages including high efficiency, cost-effectiveness, and minimal environmental impact [11,23,24].

Microalgae, unicellular microorganisms utilizing light energy and carbon dioxide for development, prove to be effective adsorbents due to their ease of cultivation and multifunctional capabilities. Microalgae not only adsorb molecules but also contribute to carbon dioxide consumption and the utilization of agricultural byproducts like phosphorous and nitrogen [25]. Despite their advantageous features, microalgae pose a growing national water threat in many developing nations due to algal blooming and eutrophication [26]. Elevated concentrations of microalgae can lead to oxygen depletion in water bodies, causing harm to aquatic life, including the death of fish. However, repurposing microalgae as adsorbents transforms this potential environmental threat into a valuable resource.

While various studies have explored heavy metal adsorption using microalgae [22,27–33], these investigations often focused on specific pH conditions—either acidic, neutral, or alkaline. For instance, Aksu et al. [28] examined Cd adsorption onto *C. vulgaris* at pH 4, reporting the maximum adsorbed concentration (q_{max}) of 770.4 mmol/kg. Hockaday et al. [34] studied the adsorption of Cd and Cu onto biomass at pH 6, obtaining q_{max} values of 98.4 mmol/kg for Cd and 400.2 mmol/kg for Cu with *C. vulgaris*, and q_{max} values of 219.90 mmol/kg for Cd and 152.6 mmol/kg for Cu with *S. obliquus*. Additionally, Bordoloi et al. [35] investigated Co adsorption by microalgae-based biochar at pH 5, yielding a q_{max} value of 11.4 mmol/kg. Given the significant impact of pH on heavy metal adsorption by microalgae, influencing the charge density of the cell wall and functional groups on cell surfaces, there is a need to characterize heavy metal adsorption mechanisms across different pH values.

This study aims to build upon prior research on heavy metal adsorption by characterizing the adsorption mechanisms of Cd^{2+}, Co^{2+}, and Cu^{2+} onto three prevalent microalgae strains (*C. vulgaris, Scenedesmus* sp., and *S. platensis*) under both acidic (pH 4) and neutral (pH 7) conditions. Utilizing the Langmuir, Freundlich, and Dubinin–Radushkevich Isotherm models, the objective is to enhance understanding of the differences in sorption mechanisms among the three microalgae strains for these cations. The inclusion of both acidic (pH 4 in this study) and neutral (pH 7) environments is crucial to account for potential Acid Mine Drainage (AMD) in effluent exposed to sulfur-enriched rocks, as well as instances where rocks lack acid-forming minerals [36].

2. Materials and Methods

2.1. Cultivation of Microalgae

Isolated species of *C. vulgaris* (KTC No. AG10052), *Scenedesmus* sp. (KTC No. AG20456), and S. *platensis* (KTC No. AG608369) were purchased from the Korean Collection for Type Cultures. *C. vulgaris* and *Scenedesmus* sp. were cultivated using Blue-Green 11 (BG-11) growth medium, which comprises $NaNO_3$, $K_2HPO_4 \cdot 3H_2O$, $MgSO_4 \cdot 7H_2O$, $CaCl_2 \cdot 2H_2O$, citric acid, ferric ammonium citrate, Na_2CO_3, and a trace metal mix containing H_3BO_3, $MnCl_2 \cdot 4H_2O$, $ZnSO_4 \cdot 7H_2O$, $Na_2MoO_4 \cdot 2H_2O$, $CuSO_4 \cdot 5H_2O$, and $Co(NO_3)_2 \cdot 6H_2O$, while *S. platensis* was cultured using Spirulina–Ogawa–Terui (SOT) growth medium, which comprises $NaHCO_3$, Na_2CO_3, $NaNO_3$, K_2HPO_4, K_2SO_4, NaCl, $MgSO_4 \cdot 7H_2O$, $CaCl_2 \cdot 2H_2O$, and a trace metal solution containing $FeSO_4 \cdot 7H_2O$ and EDTA. The microalgae strains were nurtured in photo batch reactors (PBRs) with LED strips as the light source. The LED lights were adjusted to provide continuous illumination for only 12 h each day, allowing the microalgae strains to undergo both light and dark cycles of biomass growth. The batch reactors were operated at 20 °C and continuous aeration was provided to the biomass through aeration tubes with high-efficiency particulate air filters.

2.2. Recovery and Processing of Biomass

After approximately 35 days of cultivation, the microalgae were harvested and dewatered using a centrifuge (UNION 32R PLUS, Hanil Science Co., Ltd., Daejeon, Republic of Korea). To prevent lipid expulsion from the biomass, *C. vulgaris* and *Scenedesmus* sp. underwent centrifugation at 3000 rpm for 5 min, while S. *platensis* was centrifuged at 4000 rpm for 8 min in 250 mL centrifuge tubes at 18 °C. The dewatered biomass was then washed with deionized water and dewatered again. This process was repeated three times to eliminate minerals from the growth media in the biomass. The dewatered biomass was freeze-dried at <20 Pa and −80 °C for 12 h using a freeze-dryer (Yamato scientific freeze-dryer, Tokyo, Japan). Following the freeze-drying, the biomass was ground using a motor and pestle and sieved through a 212-micron test sieve. The residue on the sieve was ground again, and the procedure was repeated until all the biomass was crushed to 0.212 mm or smaller.

2.3. FT-IR Characterisation of Biomass

Surface functional groups of the biomass were characterized using Fourier Transform Infrared (FTIR) spectrometry (Bruker Equinox 55 FT-IR spectrometer, Berlin, Germany) that was outfitted with a deuterated triglycerine sulfate detector and an HTS-XT high-throughput microplate extension. The spectral range covered was from 4000 to 400 cm^{-1}, with each spectrum being an average of four co-added scans.

2.4. Preparation of Stock Solution

$Cd(NO_3)_2 \cdot 4H_2O$, $Co(NO_3)_2 \cdot 6H_2O$, and $CuSO_4 \cdot 5H_2O$ were dissolved in deionized water to prepare 2000 mg/L Cd^{2+}, Co^{2+}, and Cu^{2+} stock solutions, respectively. The stock solutions were further diluted to the desired concentrations for subsequent experiments.

2.5. Biosorption Experiments

Biosorption isotherm experiments were carried out in 50 mL polycarbonate vials (Nalgene Co., Rochester, NY, USA). Each vial contained 0.05 g of biomass measured gravimetrically and was filled with about 50 mL of metal solution without head space to minimize unexpected oxidation. The pH of the solution was adjusted to pH4 and pH7 for acidic and neutral conditions, respectively, using HNO_3 and NaOH. The initial concentration of the metal solutions was set from 0.24 to 1.8 mmol/L for Cd^{2+}, from 0.42 to 3.45 mmol/L for Co^{2+}, and from 0.39 to 3.25 mmol/L for Cu^{2+}.

The pH edge experiment was also conducted to determine the influence of pH on the metal adsorption at a pH range from 4 to 9.5 in the metal solution with metal concentrations of 0.44, 0.85, and 0.81 mmol/L for Cd^{2+}, Co^{2+}, and Cu^{2+}, respectively. The vials containing the mixture of biomass and metal solution were tightly capped and shaken in an orbital

shaker at 120 rpm for 24 h. After mixing, the vials were centrifuged and filtered through a 0.2 µm syringe filter (Whatman, cellulose nitrate membrane filter) for analysis. The amount of metal ion (mmol/kg) adsorbed onto the biomass was calculated using the formula below:

$$q_e = \frac{(C_0 - C_e)V}{W} \quad (1)$$

where C_0 and C_e represent the initial and the equilibrium metal concentrations (mmol/L) after 24 h of shaking, respectively. q_e (mmol/kg) describes the adsorbed concentration in biomass. V represents the sample volume (L), and W represents the weight of the biomass (kg). All experiments were carried out in duplicate.

2.6. Analytic Methods

The metal concentration in the aqueous phase was measured using capillary electrophoresis (PrinCE-760, Emmen, The Netherlands), operated in the indirect capillary zone electrophoresis method (Indirect CZE). Briefly, the samples were injected into a 30 cm long silica fused capillary with a detector window at 22 cm for 6 s at 25 millibars. Thereafter, a separation voltage of 30 V was applied between the two ends of the capillary, and an analysis was run for 3 min. The buffer solution used 30 mM of glycolic acid and 10 mM of benzylamine [37].

2.7. Biosorption Isotherm Models

The Langmuir isotherm model is employed to describe the adsorption of solutes onto an adsorbent with a finite number of adsorption sites. This model assumes monolayer adsorption and a constant heat of adsorption for all the adsorption sites. The Langmuir model is written as:

$$q_e = \frac{q_{mL} b_L C_e}{1 + b_L C_e} \quad (2)$$

where q_{mL} (mmol/kg) describes the maximum adsorption capacity, b_L describes the Langmuir constant associated with site energy, and C_e (mmol/L) represents the equilibrium of heavy metal in the solution [21,22].

The Freundlich model assumes heterogeneity and exponential distribution of energy and adsorption sites. The Freundlich model is written as:

$$q_e = K_F C_e^{N_F} \quad (3)$$

where K_F [(mmol/kg)/(mmol/L)^{NF}] denotes the Freundlich sorption coefficient, C_e (mmol/L) represents the equilibrium concentration of the heavy metal post-adsorption, and N_F denotes the Freundlich exponent [22,38].

The Dubinin–Radushkevich (D-R) isotherm model [39] is used to describe the sorption of molecules onto microporous surfaces. The D-R model is written as:

$$q_e = q_{mD} \exp(-\beta\varepsilon^2) = q_{mD} \exp\left[-\beta\left(RT \ln\left(1 + \frac{1}{C_e}\right)\right)^2\right] \quad (4)$$

where q_{mD} (mmol/kg) describes the maximum adsorption capacity, $ß$ represents the activity coefficient of the sorption energy in the form (mol^2/J^2), ε is the Polanyi potential, R is the gas constant taken at a value of (8.314 J/mol/K), and T denotes the temperature in kelvins (K) [38].

$$\varepsilon = RT \ln\left(1 + \frac{1}{C}\right) \quad (5)$$

$$E = \frac{1}{\sqrt{2\beta}} \quad (6)$$

where E is the energy of sorption as described in the D-R isotherm model.

2.8. Determination of the Point of Zero Charge (pH_{pzc})

To determine the pH_{pzc}, 0.02 g of each biomass species was mixed with 50 mL of 0.1 mol/L NaCl solution. The initial pH (pH_i) of the solution was adjusted to values ranging from 2 to 12 in separate vials. After 48 h of mixing, the final pH (pH_f) of each vial was measured [22].

2.9. Determination of DOC

To ascertain the amount of dissolved organic carbon (DOC) generated by the biomass, samples from the batch reactors in each experiment were filtered. The concentration of DOC in the filtered solution was then assessed at 6 h, 12 h, and 24 h using a total organic carbon analyzer (TOC-L, Shimadzu, Kyoto, Japan).

3. Results and Discussion

3.1. Effect of pH on the Adsorption of Heavy Metals by Biomass

In Figure 1, the results are depicted concerning the point of zero charge (pH_{pzc}). It was observed that the pH_{pzc} of *C. vulgaris*, *Scenedesmus* sp., and *S. platensis* were approximately 6.96, 6.80, and 6.99, respectively. Previous studies have indicated that at pH levels below pH_{pzc}, the functional groups on the surface of biomass are tightly bound with the H_3O^+ ions in the aqueous solution [22]. However, as the pH surpasses the pH_{pzc}, the outer layer of the biomass undergoes deprotonation, exposing the negatively charged functional groups [40–42]. The exposed functional groups can then interact with heavy metals, facilitating the formation of bonds [22].

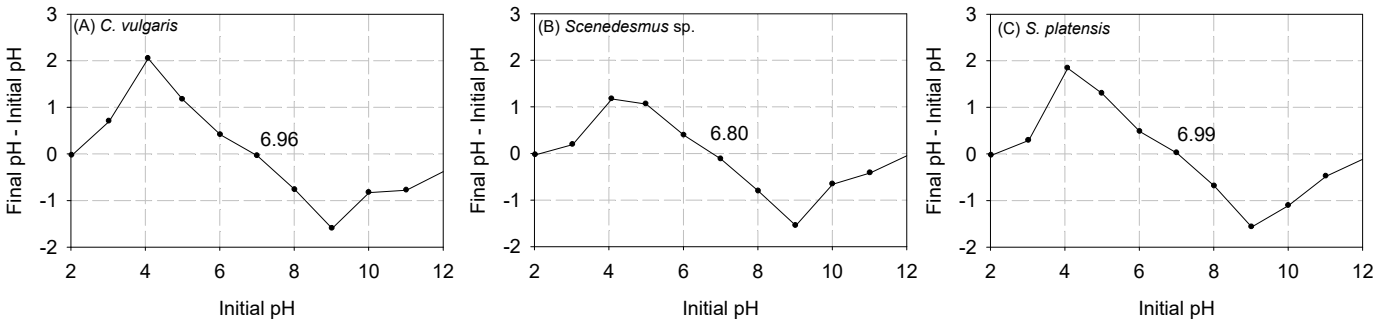

Figure 1. Results of the pH_{pzc} of (**A**) *C. vulgaris*, (**B**) *Scenedesmus* sp., and (**C**) *S. platensis*.

Furthermore, as depicted in Figure 2, the adsorption of heavy metals onto *C. vulgaris*, *Scenedesmus* sp., and *S. platensis* showed a dependence on pH. Increasing pH led to an increase in the adsorption capacity of the biomass for Cd, Co, and Cu. This effect can be attributed to higher concentrations of H_3O^+ ions in the aqueous solution at lower pH levels, which compete with heavy metal cations for available adsorption sites, consequently limiting the number of unoccupied adsorption sites on the biomass surfaces [43]. As the pH transition from acidic to alkaline, the concentration of hydronium ions in the solution decreases, reducing competition for adsorption sites. Additionally, it was noted that at pH values above 9.5, 9.0, and 7.5, precipitation, rather than adsorption, became the predominant removal mechanism for Cd, Co, and Cu, respectively.

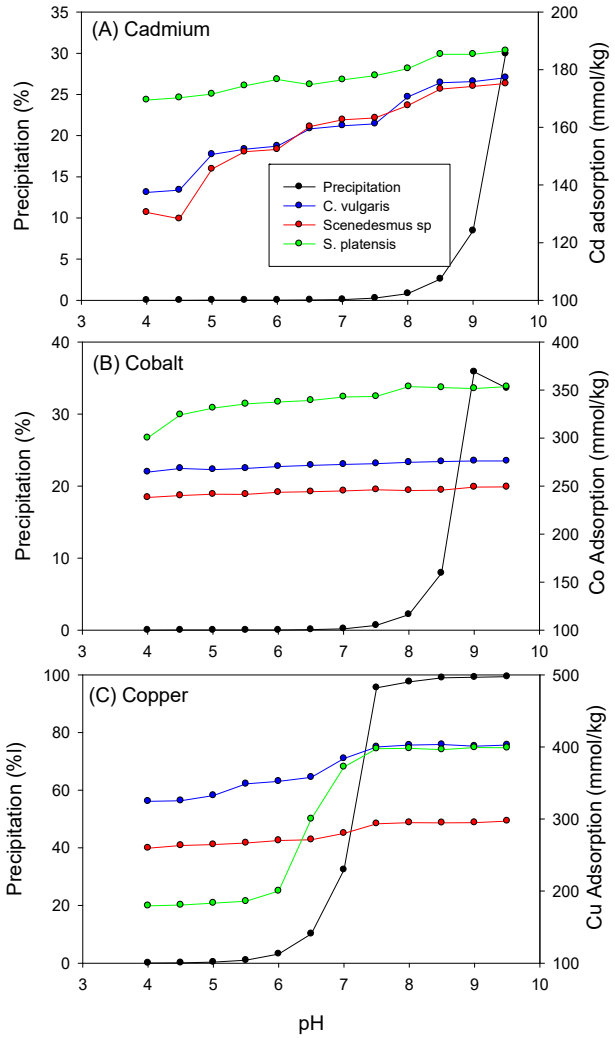

Figure 2. Influence of pH on the biosorption of (**A**) Cadmium, (**B**) Cobalt, and (**C**) Copper onto the biomass.

3.2. FTIR Spectra

The FTIR spectrum of the microalgae is illustrated in Figure 3. The band near 3300 cm^{-1} is attributed to the N-H stretching vibrations in amides related to proteins and the O-H stretching in water [44]. The region between 2800 cm^{-1} and 3000 cm^{-1} is indicative of the stretching vibrations of aliphatic C-H groups found in lipids and proteins, as well as the asymmetric stretching of aldehydes [45]. The band at 1650 cm^{-1} corresponds to the C=O stretching vibrations in protein-associated amides [44]. The peak at 1527 cm^{-1} is due to the C-N and N-H stretching vibrations in proteins, whereas the peak at 1470 cm^{-1} is associated with C=C stretching [44]. After adsorption, slight changes were observed for all three strains of microalgae, between wavenumbers corresponding to the O-H groups, the amine and amide groups, carboxyl functional groups, and C-O vibrations in the hydroxyl groups.

The spectra provide insight into the functional groups involved in the biosorption process. For instance, the intensity and position of the O-H and carboxyl group peaks showed noticeable shifts, indicating their involvement in the biosorption process. Specifically, the peak corresponding to the O-H stretching vibration showed a slight shift in all three strains of biomass after adsorption, suggesting interactions between the metal ions and hydroxyl groups on the biomass surface. These spectral changes imply the formation of metal–oxygen and metal–nitrogen bonds, corroborating the involvement of hydroxyl, carboxyl, and amine groups in the metal binding process. The shifts in wavenumber and

changes in peak intensity confirm that functional groups on the biomass surface play a crucial role in the adsorption of heavy metals.

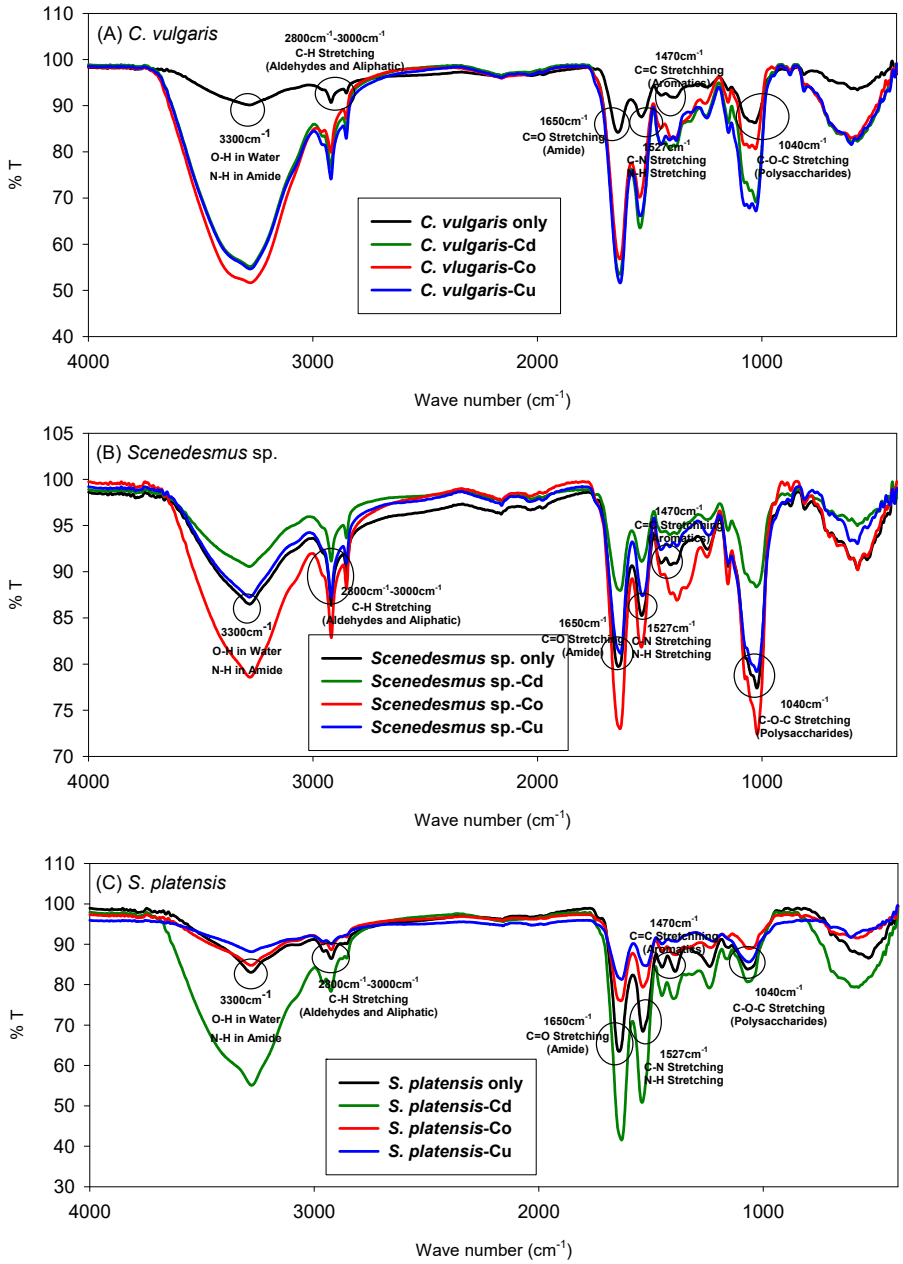

Figure 3. FT-IR spectra of (**A**) *C. vulgaris*, (**B**) *Scenedesmus* sp., and (**C**) *S. platensis* before and after biosorption of Cd^{2+}, Co^{2+}, and Cu^{2+}.

3.3. Biosorption under Acidic Conditions

The adsorption data of Cd, Co, and Cu exhibited good fits ($0.87 < R^2 < 0.99$) across all isotherm models tested with *C. vulgaris*, *Scenedesmus* sp., and *S. platensis* under acidic conditions. Figure 4 and Table 1 show the biosorption isotherms and sorption parameters of Cd, Co, and Cu onto C. *vulgaris* under acidic conditions, respectively. The adsorption of metal ions onto biomass was analyzed using the Langmuir model [42,43], which assumes monolayer adsorption on homogeneous surfaces. The determination coefficient (R^2) values for Cd, Co, and Cu obtained from the Langmuir model exceeded those from the Freundlich model, indicating that the sorption of the cations onto *C. vulgaris* under acidic conditions was predominantly homogenous. The Langmuir model estimated the maximum

adsorption capacity (q_{mL}) for *C. vulgaris* in the following order: Co (2172 mmol/kg) > Cu (1917 mmol/kg) > Cd (1175 mmol/kg). The R_L parameter of the Langmuir model indicates the favorability of adsorption. It encompasses various scenarios: unfavorability ($R_L > 1$), linearity ($R_L = 1$), and favorability ($0 < R_L < 1$) [38]. In this study, the R_L values were computed at the maximum initial concentration, and all produced values were consistent with $R_L < 1$, indicating that the sorption of Cd, Co, and Cu onto *C. vulgaris* under acidic conditions was favorable.

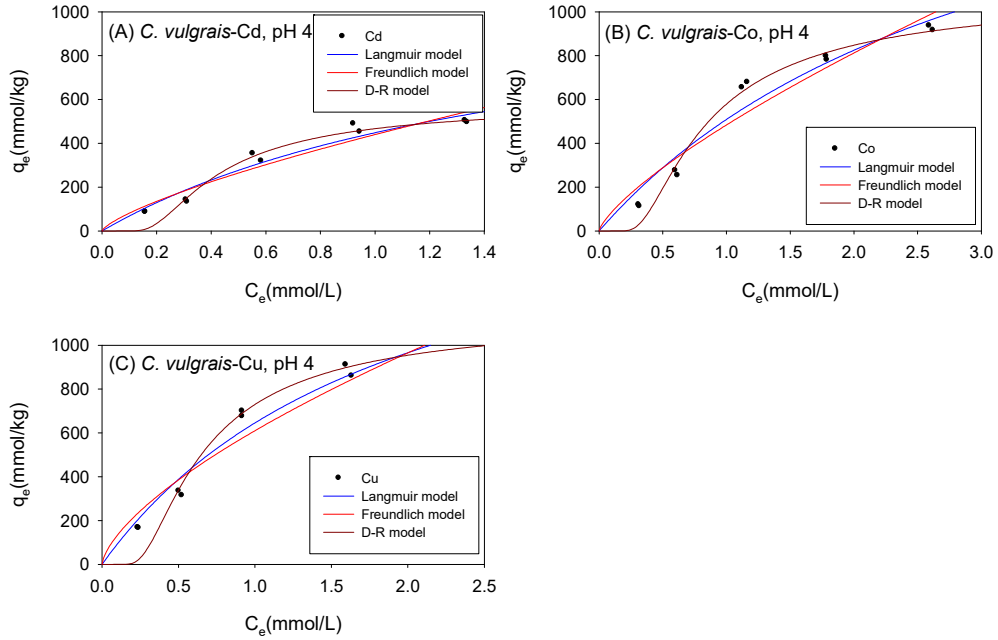

Figure 4. Isotherm results of the adsorption of (**A**) Cd^{2+}, (**B**) Co^{2+}, and (**C**) Cu^{2+} onto C. *vulgaris* under acidic conditions.

Table 1. Comparison of the isotherm parameters for *C. vulgaris* under acidic conditions.

Model	Parameter	Cd	Co	Cu
Langmuir	q_{mL} (mmol/kg)	1175	2172	1917
	b_L (L/mmol)	0.617	0.306	0.507
	R^2	0.947	0.95	0.97
	SSE	2434	14,430	5475
	R_L	0.474	0.487	0.377
Freundlich	K_F ($mmol^{1-N}L^N/kg$)	439.7	483.7	609.8
	N(-)	1.363	1.338	1.51
	R^2	0.923	0.925	0.944
	SSE	1375	7322	4111
D-R	q_{mD} (mmol/kg)	647.7	1383	1347
	K_{dr} (mol^2/J^2)	1.380×10^{-8}	3.669×10^{-8}	2.584×10^{-8}
	R^2	0.945	0.978	0.953
	SSE	18,700	16,274	62,132
	E (kJ/mol)	6.019	3.691	4.4

The Freundlich model has been also employed to describe the sorption of cations onto biomass [34]. It incorporates the heterogeneity of the adsorbent and the exponential distribution of the active sites and their corresponding energies. The K_F values in the Freundlich model describe the adsorption affinity of the adsorbent for the sorbent. As depicted in Table 1, the K_F values for *C. vulgaris* under acidic conditions followed the order Cu (609.8 $mmol^{1-N}L^N/kg$) > Co (483.7 $mmol^{1-N}L^N/kg$) > Cd (439.8 $mmol^{1-N}L^N/kg$).

The D-R model is mostly utilized for characterizing the sorption of molecules and ions onto microporous surfaces [38]. While some researchers have applied the D-R model to elucidate cation adsorption onto microalgae, most researchers have focused on the Langmuir and Freundlich isotherm models. However, studies that employed the D-R model to fit their isotherm data revealed that this model could indeed be used to describe the adsorption of metal ions onto biomass [33]. One advantage that the D-R model offers over the Langmuir and Freundlich models is that it provides an estimate of the sorption energy (E), which may be used to predict the mechanisms involved in adsorption. When E is between 8 kJ/mol and 16 kJ/mol, the sorption mechanism is predominantly ion exchange; when E is less than 8 kJ/mol, the sorption mechanism is predominantly physical in nature; moreover, when E is greater than 16 kJ/mol, the sorption mechanism is described as chemical sorption. As presented in Table 1, it was observed that the sorption mechanism involved in the adsorption of Cd, Co, and Cu onto *C. vulgaris* under acidic conditions is predominantly physical in nature. Studies have demonstrated that physical sorption mainly occurs due to weak van der Waals forces [38]. The q_{mD} parameter of the D-R model may also be used to describe the maximum adsorption capacity (q_{max}) of the metal ions onto biomass. The q_{max} values of *C. vulgaris* for Cd, Co, and Cu are 648 mmol/kg, 1383 mmol/kg, and 1347 mmol/kg, respectively.

As observed in Table 1, there was a discrepancy between the q_{mD} and q_{mL} values. This difference is attributed to the fact that the Langmuir model considers the adsorption of metal ions onto the monolayer surface of the biomass to compute the q_{mL}, while the D-R model computes the q_{mD} by considering the amount of heavy metal ions adsorbed into the micro-pores of the biomass [46]. The determination coefficients (R^2) of the Langmuir and the D-R model for each metal were compared to determine which isotherm model provided a more accurate estimate of the actual maximum adsorption capacity (q_{max}).

The relatively high R^2 values obtained using the D-R model in this study were explained by the fact that microalgae cell walls have a fibrillary and amorphous structure, resulting in a sandy-like structure [33].

Figure 5 and Table 2 show the biosorption isotherms and sorption parameters of Cd, Co, and Cu onto *Scenedesmus* sp. under acidic conditions, respectively. The maximum adsorption capacity values (q_{mL}) obtained from the Langmuir model were in the order Co (2182 mmol/kg) > Cu (2070 mmol/kg) > Cd (1027 mmol/kg). Although both the D-R model and the Langmuir model yielded the maximum adsorption capacity of the adsorbed metal ions onto *Scenedesmus* sp. in the same order from highest to lowest ($Co^{2+} > Cu^{2+} > Cd^{2+}$), the D-R model estimated the amount of metal ions adsorbed to be 593 mmol/kg, 1398 mmol/kg, and 1474 mmol/kg for Cd^{2+}, Co^{2+}, and Cu^{2+}, respectively. It was observed that the adsorption isotherms of Co^{2+} and Cu^{2+} were better fitted with the D-R model with R^2 values of 0.97 for Co and 0.95 for Cu, compared to 0.90 for Co and 0.92 for Cu with the Langmuir model. It was, therefore, assumed that the q_{mD} parameter provided a more accurate estimate of the actual maximum adsorption capacity of Co and Cu onto *Scenedesmus* sp. under acidic conditions.

The higher the value of the Langmuir model parameter b_L, the more the adsorbent surface is coated with firmly attached sorbate molecules. In this study, the b_L parameters showed that, in acidic conditions, Cd ions were more tightly attached to *Scenedesmus* sp. biomass than Cu and Co cations. As presented in Table 2, the K_F parameters described the sorption affinity of the cations towards *Scenedesmus* sp. to be in the order of Cu > Co > Cd, and this was the same order observed with C. *vulgaris* under acidic conditions. The Freundlich model described favorable sorption of Cd, Co, and Cu onto *Scenedesmus* sp., with N values in the range of $0.1 < 1/N < 1$. This was consistent with the Langmuir isotherm model, which also described favorable sorption for all the examined cations onto *Scenedesmus* sp. with R_L values corresponding to $0 < R_L < 1$. The sorption energy of Cd, Co, and Cu, as obtained using the D-R model, was 6.178 kJ/mol, 3.609 kJ/mol, and 3.894 kJ/mol, respectively. These findings showed that the sorption of the studied cations onto *Scenedesmus* sp. Under acidic circumstances is mostly physisorption.

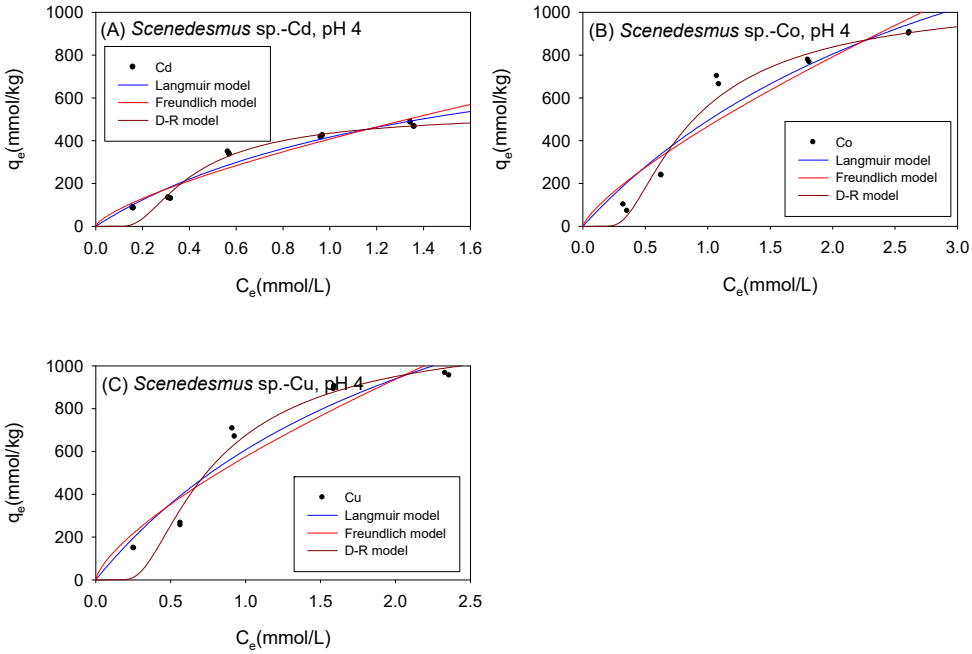

Figure 5. Isotherm results of the adsorption of (**A**) Cd^{2+}, (**B**) Co^{2+}, and (**C**) Cu^{2+} onto *Scenedesmus* sp. Under acidic conditions.

Table 2. Comparison of the isotherm parameters for *Scenedesmus* sp. Under acidic conditions.

Model	Parameter	Cd	Co	Cu
Langmuir	q_{mL} (mmol/kg)	1027	2182	2070
	b_L (L/mmol)	0.682	0.292	0.415
	R^2	0.946	0.899	0.92
	SSE	1773	25,008	13,751
	R_L	0.449	0.498	0.426
Freundlich	K_F ($mmol^{1-N}L^N/kg$)	407.7	466.4	575.3
	N(-)	1.407	1.31	1.421
	R^2	0.923	0.873	0.889
	SSE	1026	1111	7448
D-R	q_{mD} (mmol/kg)	592.8	1398	1474
	K_{dr} (mol^2/J^2)	1.310×10^{-8}	3.839×10^{-8}	3.290×10^{-8}
	R^2	0.945	0.97	0.948
	SSE	14,720	1920	46,868
	E (kJ/mol)	6.178	3.609	3.894

Figure 6 and Table 3 show the biosorption isotherms and sorption parameters of Cd, Co, and Cu onto S. *platensis* under acidic conditions, respectively. According to the q_{mL} parameters, the maximum sorption capacity of the metal ions onto *S. platensis* was 1034 mmol/kg, 1768 mmol/kg, and 3503 mmol/kg for Cd, Co, and Cu, respectively. On the other hand, the q_{mD} parameter estimated the maximum adsorption capacity to be 639 mmol/kg for Cd, 1359 mmol/kg for Co, and 1754 mmol/kg for Cu. With the exception of Cu, the adsorption isotherms were better fitted with the Langmuir model. The sorption energies of all the cations were less than 8 kJ/mol, indicating that physical sorption was the primary sorption process involved in cation sorption onto *S. platensis* unlike *C. vulgaris* and *Scenedesmus* sp., where the biomass' affinity towards the cations as indicated by the K_F parameter was in the order Cu > Co > Cd; moreover, it was observed that *S. platensis*'s sorption affinity for the cations under acidic conditions was in the order of Co > Cu > Cd.

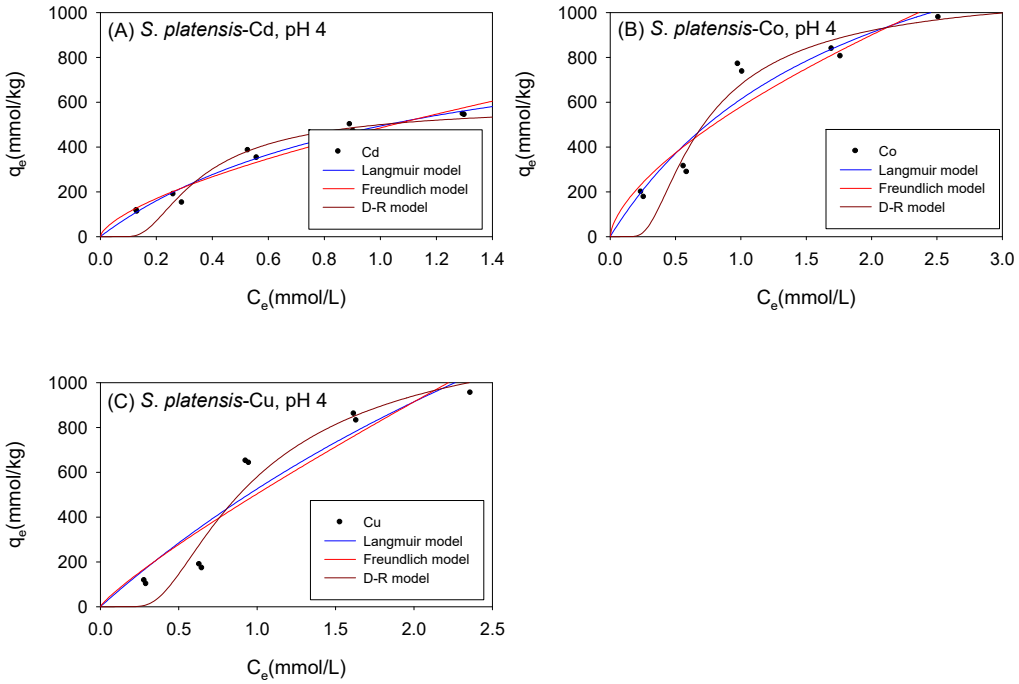

Figure 6. Isotherm results of the adsorption of (**A**) Cd^{2+}, (**B**) Co^{2+}, and (**C**) Cu^{2+} onto *S. platensis* under acidic conditions.

Table 3. Comparison of the adsorption isotherm parameters for *S. platensis* under acidic conditions.

Model	Parameter	Cd	Co	Cu
Langmuir	q_{mL} (mmol/kg)	1034	1768	3503
	b_L (L/mmol)	0.913	0.531	0.177
	R^2	0.969	0.926	0.895
	SSE	291.1	3,449	22,557
	R_L	0.378	0.351	0.635
Freundlich	K_F ($mmol^{1-N}L^N/kg$)	485.3	579.6	503.7
	N(-)	1.532	1.576	1.163
	R^2	0.95	0.9	0.882
	SSE	537.7	3028	1001
D-R	q_{mD} (mmol/kg)	638.6	1359	1754
	K_{dr} (mol^2/J^2)	1.033×10^{-8}	2.923×10^{-8}	4.662×10^{-8}
	R^2	0.901	0.905	0.943
	SSE	39,385	80,097	21,410
	E (kJ/mol)	6.957	4.136	3.275

3.4. Comparison of the Maximum Adsorption Capacities of the Cations onto Biomass under Acidic Condition

Figure 7 shows a comparison of the maximum adsorption capacities of Cd, Co, and Cu onto *C. vulgaris*, *Scenedesmus* sp., and *S. platensis* in acidic settings. Here, only the q_{max} values associated with the isotherm model with a higher determination coefficient between the Langmuir and D-R models are displayed. It was observed that the sorption of the heavy metal ions onto biomass (mmol/kg) was in the order of Cu > Co > Cd. It is assumed that the similarity in the sorption pattern results from shared characteristics of microalgae, such as functional groups on the cell surfaces, physical characteristics, and cell composition [45].

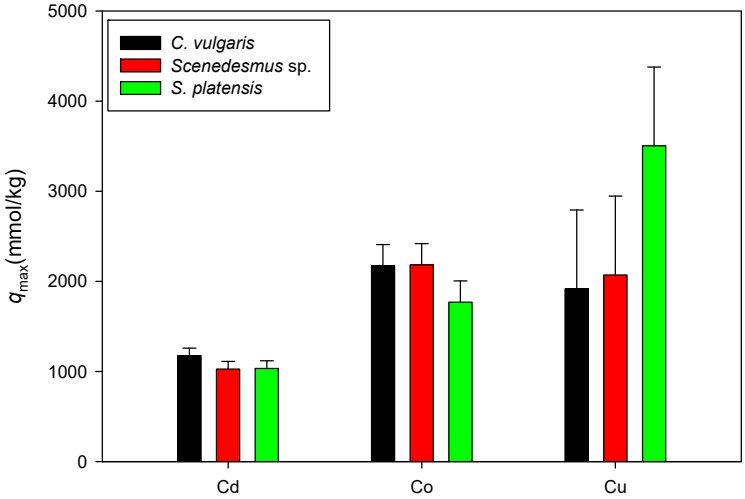

Figure 7. Comparison of q_{max} values for cation sorption onto biomass under acidic conditions.

3.5. Biosorption under Neutral Conditions

The adsorption of Cd, Co, and Cu fitted well ($0.81 < R^2 \leq 0.99$) to all the isotherm models with *C. vulgaris*, *Scenedesmus* sp., and *S. platensis* under neutral conditions.

Figure 8 and Table 4 show the biosorption isotherms and sorption parameters of Cd, Co, and Cu onto C. *vulgaris* under neutral conditions, respectively. The q_{max} values as computed using the Langmuir model were 1012 mmol/kg for Cd, 2007 mmol/kg for Co, and 2318 mmol/kg for Cu. The D-R model, on the other hand, estimated q_{max} values of 643 mmol/kg, 1424 mmol/kg, and 1558 mmol/kg for Cd, Co, and Cu respectively. With the exception of Co cations, the sorption isotherms were observed to have fitted better with the Langmuir model than the D-R model.

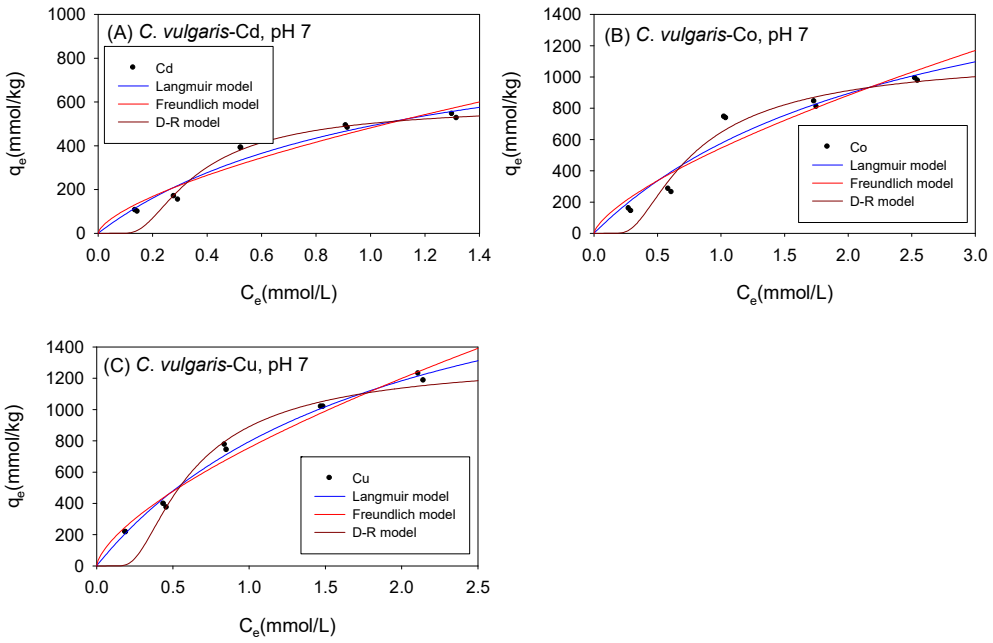

Figure 8. Isotherm results of the adsorption of (**A**) Cd^{2+}, (**B**) Co^{2+}, and (**C**) Cu^{2+} onto *C. vulgaris* under neutral conditions.

Table 4. Comparison of the adsorption isotherm parameters for *C. vulgaris* under neutral conditions.

Model	Parameter	Cd	Co	Cu
Langmuir	q_{mL} (mmol/kg)	1012	2007	2318
	b_L (L/mmol)	0.941	0.402	0.522
	R^2	0.951	0.921	0.99
	SSE	1867	11,272	526.1
	R_L	0.371	0.419	0.371
Freundlich	K_F ($mmol^{1-N}L^N/kg$)	481.5	544.6	755.7
	N(-)	1.531	1.438	1.501
	R^2	0.92	0.893	0.977
	SSE	1259	6159	2057
D-R	q_{mD} (mmol/kg)	642.6	1424	1558
	K_{dr} (mol^2/J^2)	1.041×10^{-8}	3.334×10^{-8}	2.359×10^{-8}
	R^2	0.939	0.942	0.926
	SSE	22,382	34,713	168,086
	E (kJ/mol)	6.93	3.873	4.604

For all the cations, the sorption affinity denoted by the Freundlich model parameter K_F was higher in the experiments conducted under neutral conditions than in studies conducted under acidic settings. Likewise, as the environment changed from acidic to neutral, the binding capacity denoted by the Langmuir model parameter b_L increased. The rise in sorption affinity and binding capacity in neutral settings was attributed to the decrease in H_3O^+ concentration with an increase in pH. Moreover, in neutral settings, the functional groups on *C. vulgaris* were deprotonated, thereby, facilitating the binding of the heavy metals onto biomass [43].

Even with the shift from acidic to neutral settings, the energy of sorption denoted by the D-R model parameter E remained below 8 kJ/mol, indicating that the sorption mechanism of Cd, Co, and Cu onto *C. vulgaris* is largely physical in nature in neutral conditions, just as in acidic conditions.

Figure 9 and Table 5 show the biosorption isotherms and sorption parameters of Cd, Co, and Cu onto *Scenedesmus* sp. under neutral conditions, respectively. The q_{max} values as computed using the Langmuir model were 1044 mmol/kg for Cd, 2070 mmol/kg for Co, and 2037 mmol/kg for Cu. The D-R model, on the other hand, estimated q_{max} values of 606 mmol/kg, 1389 mmol/kg, and 1332 mmol/kg for Cd, Co, and Cu, respectively. With respect to the determination coefficient (R^2), the Langmuir model produced a much more accurate estimate of the q_{max} for Cd and Cu, whereas the D-R model estimated the q_{max} for Co better.

As with C. *vulgaris*, similar trends were observed in the sorption mechanism of the cations onto *Scenedesmus* sp., with a change from acidic to neutral environments. The binding capacity (b_L) of the cations increased with a shift in the environment from 0.68 (L/mmol) to 0.81 (L/mmol), 0.29 (L/mmol) to 0.34 (L/mmol), and 0.42 (L/mmol) to 0.59 (L/mmol) for Cd^{2+}, Co^{2+} and Cu^{2+}, respectively. The sorption affinity (K_F) of *Scenedesmus* sp. also increased with a shift in the environment. Furthermore, as with *C. vulgaris*, physical sorption remained the primary sorption mechanism of the cations onto *Scenedesmus* sp. despite switching from acidic to neutral settings.

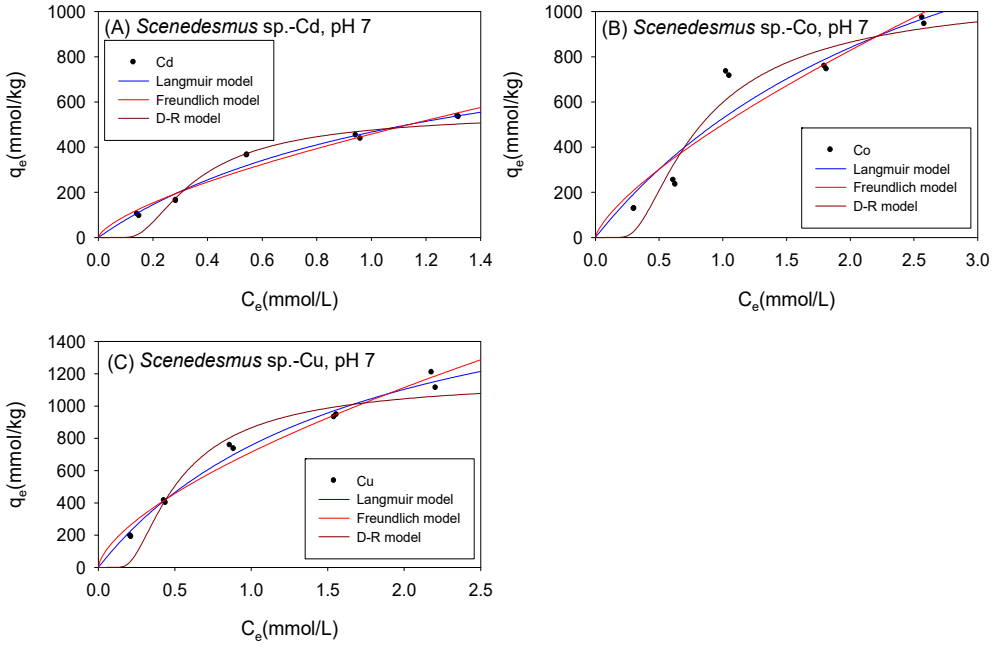

Figure 9. Isotherm results of the adsorption of (**A**) Cd^{2+}, (**B**) Co^{2+}, and (**C**) Cu^{2+} onto *Scenedesmus* sp. under neutral conditions.

Table 5. Comparison of the adsorption isotherm parameters for *Scenedesmus* sp. under neutral conditions.

Model	Parameter	Cd	Co	Cu
Langmuir	q_{mL} (mmol/kg)	1044	2070	2037
	b_L (L/mmol)	0.808	0.342	0.591
	R^2	0.975	0.894	0.986
	SSE	724	12,638	1486
	R_L	0.408	0.459	0.343
Freundlich	K_F ($mmol^{1-N}L^N/kg$)	457.7	500.1	713.868
	N(-)	1.471	1.374	1.556
	R^2	0.958	0.872	0.972
	SSE	637.9	6280	2376.231
D-R	q_{mD} (mmol/kg)	605.8	1389	1332
	K_{dr} (mol^2/J^2)	1.021×10^{-8}	3.550×10^{-8}	1.819×10^{-8}
	R^2	0.934	0.927	0.929
	SSE	18,822	17,851	62,185
	E (kJ/mol)	6.998	3.753	5.243

Figure 10 and Table 6 show the biosorption isotherms and sorption parameters of Cd, Co, and Cu onto *S. platensis* under neutral conditions, respectively. The Langmuir model computed q_{max} values of 887 mmol/kg for Cd, 1790 mmol/kg for Co, and 1824 mmol/kg for Cu. The D-R model, in contrast, estimated q_{max} values of 625 mmol/kg, 1349 mmol/kg, and 1318 mmol/kg for Cd, Co, and Cu, respectively. Compared to the D-R model, the R^2 was higher with the Langmuir model for all the cations, implying that the q_{max} indicated by the Langmuir model was a much more reliable estimate. The Langmuir model appeared to fit the Co and Cu isotherm data better than the Freundlich model, whereas the Cd isotherm data fitted better with the Freundlich model.

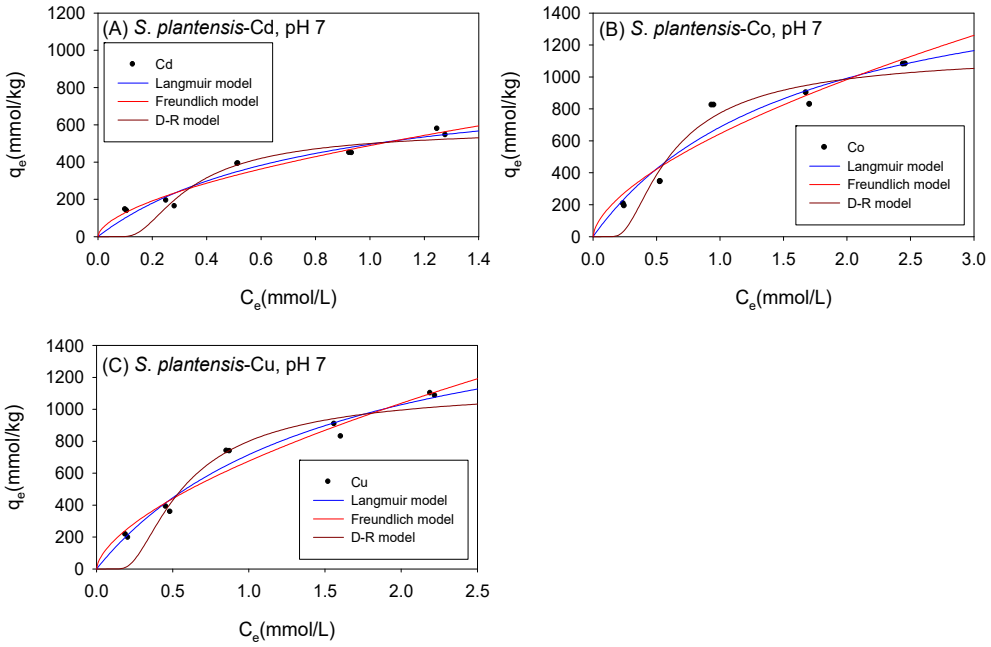

Figure 10. Isotherm results of the adsorption of (**A**) Cd^{2+}, (**B**) Co^{2+}, and (**C**) Cu^{2+} onto *S. platensis* under neutral conditions.

Table 6. Comparison of the adsorption isotherm parameters for *S. platensis* under neutral conditions.

Model	Parameter	Cd	Co	Cu
Langmuir	q_{mL} (mmol/kg)	886.7	1790	1824
	b_L (L/mmol)	1.267	0.621	0.646
	R^2	0.942	0.925	0.969
	SSE	677.5	5081	357.2
	R_L	0.305	0.319	0.323
Freundlich	K_F ($mmol^{1-N}L^N/kg$)	488.6	643.8	675.4
	N(-)	1.718	1.636	1.616
	R^2	0.943	0.897	0.956
	SSE	12.82	3782	1405
D-R	q_{mD} (mmol/kg)	624.6	1349	1318
	K_{dr} (mol^2/J^2)	9.397×10^{-9}	2.344×10^{-8}	2.104×10^{-8}
	R^2	0.812	0.911	0.902
	SSE	76,511	58,372	117,988
	E (kJ/mol)	7.294	4.619	4.875

Just as with *C. vulgaris* and *Scenedesmus* sp., *S. platensis*' sorption affinity (K_F) for the cations increased in neutral settings. Additionally, the sorption mechanism remained unaltered as the D-R model generated sorption energy values (E), corresponding to physio-sorption.

3.6. Comparison of the Maximum Adsorption Capacities of the Cations onto Biomass under Neutral Conditions

Figure 11 shows a comparison of the maximum adsorption capacities of Cd, Co, and Cu onto *C. vulgaris*, *Scenedesmus* sp., and *S. platensis* in neutral settings. Here, only the q_{max} values associated with the isotherm model with a higher R^2 between the Langmuir and D-R are displayed. Similar to the experiments in acidic settings, it was observed that the sorption of the cations onto biomass under neutral conditions was in the order Cu > Co > Cd.

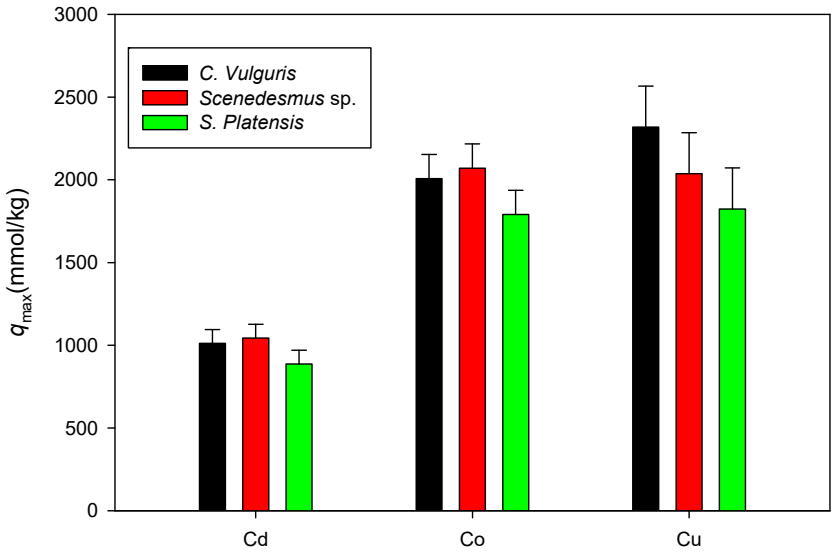

Figure 11. Comparison of q_{max} values for cation sorption onto biomass under neutral conditions.

3.7. The Effect of Sorption on the Concentration of Dissolved Carbon

Despite a strain of microalgae having a high maximum adsorption capacity for a particular cation, it is necessary to additionally analyze the bi-products of the biosorption process since they might occasionally be toxic and negate the benefits of adsorption. Sun et al. [22] reported that the dissolved organic carbon (DOC) produced by microalgae during adsorption could further react with chlorine to form haloacetic acids (HAAs) and trihalomethanes (THMs). HAAs and THMs have been associated with a variety of disorders, including cancer and reproductive health issues; they are classified as potential or possible human carcinogens and are thus controlled by several environmental protection agencies across the world [47]. Additionally, high DOC in water can cause aesthetic concerns as well as raising the risk of microbial recurrence in the water supply network [48].

Figure 12 depicts the influence of cation and adsorption time on the amount of DOC generated by *C. vulgaris*, *Scenedesmus* sp., and *S. platensis* in both acidic and neutral environments. The amount of DOC produced by biomass after 24 h of experimentation was in the following order: *S. platensis* > *Scenedesmus* sp. > *C. vulgaris*. When the experiments were performed with *S. platensis*, it was observed that the solution's color progressively changed to blueish-purple. This change in color was attributed to the release of the protein phycocyanin, which is believed to have been the source of the high amount of DOC produced by *S. platensis*.

It was also noted that the experiments under acidic conditions produced more DOC than the experiments under neutral conditions; this might have been due to cell disruption of the biomass at low pH. In both acidic and neutral environments, the biomass seemed to generate the most DOC in the presence of Co^{2+}, followed by Cd^{2+}. However, it was interesting to observe that the presence of Cu^{2+} suppressed the production of DOC as the control experiments produced more DOC than the biomass spiked with Cu^{2+}.

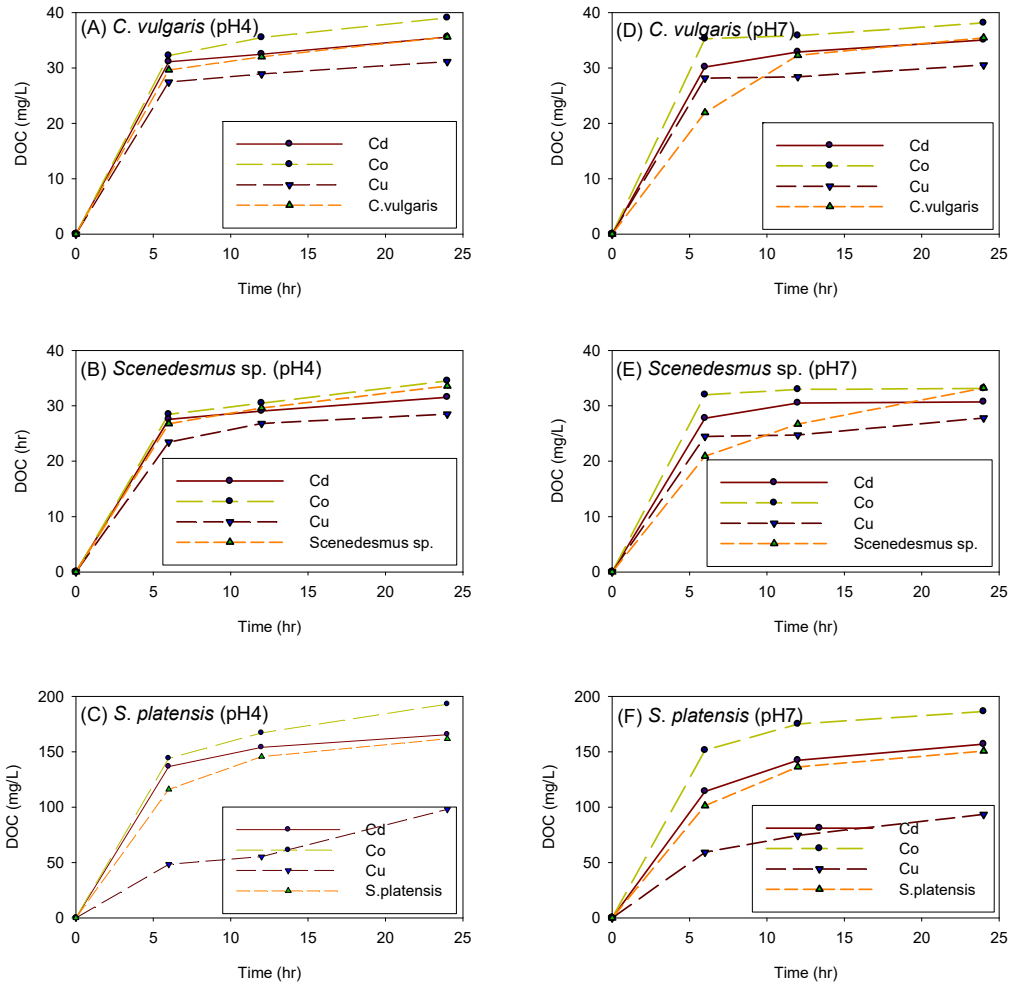

Figure 12. Influence of cation and adsorption time on the amount of DOC generated by *C. vulgaris* (**A**,**D**), *Scenedesmus* sp. (**B**,**E**), and *S. platensis* (**C**,**F**) at pH 4 and 7, respectively.

4. Conclusions

The biosorption of Cd, Co, and Cu onto *C. vulgaris*, *Scenedesmus* sp., and *S. platensis* in acidic and neutral environments was studied using the Langmuir, Freundlich, and Dubinin-Radushkevich isotherm models. For all the investigated strains of microalgae, it was found that the sorption affinity of the biomass for the metal ions was higher in neutral than in acidic environments. In both acidic and neutral settings, the sorption affinity for Cd and Co onto biomass was in the order of *S. platensis* > *C. vulgaris* > *Scenedesmus* sp., while, for Cu, the order was *C. vulgaris* > *Scenedesmus* sp. > *S. platensis*. The heavy metals Co and Cd were largely present as cations in the solution in both acidic and neutral settings, whereas Cu primarily occurred as a cation in acidic environments and as both a cation and metal precipitate in neutral settings. The maximum adsorption capacity of the heavy metals onto biomass was in the order of Cu > Co > Cd. The Dubinin-Radushkevich model described the sorption mechanism of all the metals onto biomass to be physical in nature. DOC was generated as a byproduct of the sorption of heavy metals. Generally, the amount of DOC generated under acidic conditions was higher than under neutral conditions. *S. platensis* generated the most DOC, followed by *Scenedesmus* sp., while *C. vulgaris* produced the least amount of DOC. In comparison to the control experimental settings, both Cd and Cu sorption appeared to enhance the quantity of DOC generated by biomass, whereas Cu sorption suppressed the production of DOC by biomass.

These findings are significant as they highlight the potential of using microalgae as low-cost and efficient biosorbents for heavy metal removal in varying environmental conditions. The generation of DOC as a byproduct is particularly noteworthy, as it can

influence the overall effectiveness and environmental impact of the biosorption process. Understanding the behavior of DOC under different conditions can help in optimizing biosorption processes for industrial applications. This study underscores the importance of selecting appropriate microalgae strains and environmental settings to maximize heavy metal removal and manage byproduct formation, thereby contributing valuable insights into sustainable wastewater treatment practices.

Author Contributions: J.T.P. and S.O.; methodology, J.T.P.; formal analysis, J.T.P.; investigation, J.T.P.; resources, J.T.P.; data curation, J.T.P.; writing—original draft preparation, J.T.P.; writing—review and editing, S.O.; supervision, S.O. All authors have read and agreed to the published version of the manuscript.

Funding: This research was funded by Korea Research Foundation, grant number NRF-2018R1D1A1B 07049783.

Institutional Review Board Statement: Not applicable.

Informed Consent Statement: Not applicable.

Data Availability Statement: Data are contained within the article.

Acknowledgments: This study was conducted as part of Jesse T. Phiri's master's dissertation.

Conflicts of Interest: The authors declare no conflicts of interest.

References

1. Tchounwou, P.B.; Yedjou, C.G.; Patlolla, A.K.; Sutton, D.J. Heavy Metal Toxicity and the Environment. In *Molecular, Clinical and Environmental Toxicology*; Experientia Supplementum; Springer: Basel, Switzerland, 2012; Volume 101, pp. 133–164. [CrossRef]
2. Deng, S.; Zhang, X.; Zhu, Y.; Zhuo, R. Recent Advances in Phyto-Combined Remediation of Heavy Metal Pollution in Soil. *Biotechnol. Adv.* **2024**, *72*, 108337. [CrossRef]
3. Sharpe, S.; Lenton, T.M. Are We on the Brink of an Electric Vehicle Boom? Only with More Action. *Clim. Policy* **2021**, *21*, 421–433. [CrossRef]
4. Mohtasham, J. Review Article—Renewable Energies. *Energy Procedia* **2015**, *74*, 1289–1297. [CrossRef]
5. Solangi, K.H.; Islam, M.R.; Saidur, R.; Rahim, N.A.; Fayaz, H. A Review on Global Solar Energy Policy. *Renew. Sustain. Energy Rev.* **2011**, *15*, 2149–2163. [CrossRef]
6. Jeyaseelan, C.; Jain, A.; Khurana, P.; Kumar, D.; Thatai, S. Ni-Cd Batteries. In *Rechargeable Batteries: History, Progress, and Applications*; Scrivener Publishing LLC: Austin, TX, USA, 2020; pp. 177–194. [CrossRef]
7. Stanley, A.G. Cadmium Sulfide Solar Cells. *Appl. Solid State Sci.* **1975**, *5*, 251–366. [CrossRef]
8. DeCarlo, S.; Matthews, D. More than a Pretty Color: The Renaissance of the Cobalt Industry. *J. Int. Commer. Econ.* **2019**, *2019*, 1–23.
9. Iglesias-Émbil, M.; Valero, A.; Ortego, A.; Villacampa, M.; Vilaró, J.; Villalba, G. Raw Material Use in a Battery Electric Car—A Thermodynamic Rarity Assessment. *Resour. Conserv. Recycl.* **2020**, *158*, 104820. [CrossRef]
10. Machura, P.; Li, Q. A Critical Review on Wireless Charging for Electric Vehicles. *Renew. Sustain. Energy Rev.* **2019**, *104*, 209–234. [CrossRef]
11. Chen, L.; Zhang, X.; Zhang, M.; Zhu, Y.; Zhuo, R. Removal of Heavy-Metal Pollutants by White Rot Fungi: Mechanisms, Achievements, and Perspectives. *J. Clean. Prod.* **2022**, *354*, 131681. [CrossRef]
12. Kogel, J.E. Sustainable Development and the Minerals Industry. In *Engineering Solutions for Sustainability: Materials and Resources II*; Springer: Cham, Switzerland, 2016; pp. 25–34. [CrossRef]
13. Custodio, M.; Cuadrado, W.; Peñaloza, R.; Montalvo, R.; Ochoa, S.; Quispe, J. Human Risk from Exposure to Heavy Metals and Arsenic in Water from Rivers with Mining Influence in the Central Andes of Peru. *Water* **2020**, *12*, 1946. [CrossRef]
14. Delgado, A.; Fernandez, A.; Chirinos, B.; Barboza, G.; Huamaní, E.L. Impact of the Mining Activity on the Water Quality in Peru Applying the Fuzzy Logic with the Grey Clustering Method. *IJACSA Int. J. Adv. Comput. Sci. Appl.* **2021**, *12*, 348–357. [CrossRef]
15. Muma, D.; Besa, B.; Manchisi, J.; Banda, W. Effects of Mining Operations on Air and Water Quality in Mufulira District of Zambia: A Case Study of Kankoyo Township. *J. S. Afr. Inst. Min. Metall.* **2020**, *120*, 287–298. [CrossRef]
16. Atibu, E.K.; Devarajan, N.; Laffite, A.; Giuliani, G.; Salumu, J.A.; Muteb, R.C.; Mulaji, C.K.; Otamonga, J.P.; Elongo, V.; Mpiana, P.T.; et al. Assessment of Trace Metal and Rare Earth Elements Contamination in Rivers around Abandoned and Active Mine Areas. The Case of Lubumbashi River and Tshamilemba Canal, Katanga, Democratic Republic of the Congo. *Geochemistry* **2016**, *76*, 353–362. [CrossRef]
17. Atibu, E.K.; Lacroix, P.; Sivalingam, P.; Ray, N.; Giuliani, G.; Mulaji, C.K.; Otamonga, J.P.; Mpiana, P.T.; Slaveykova, V.I.; Poté, J. High Contamination in the Areas Surrounding Abandoned Mines and Mining Activities: An Impact Assessment of the Dilala, Luilu and Mpingiri Rivers, Democratic Republic of the Congo. *Chemosphere* **2018**, *191*, 1008–1020. [CrossRef]
18. Järup, L. Hazards of Heavy Metal Contamination. *Br. Med. Bull.* **2003**, *68*, 167–182. [CrossRef]

19. Boonamnuayvitaya, V.; Chaiya, C.; Tanthapanichakoon, W.; Jarudilokkul, S. Removal of Heavy Metals by Adsorbent Prepared from Pyrolyzed Coffee Residues and Clay. *Sep. Purif. Technol.* **2004**, *35*, 11–22. [CrossRef]
20. Shamsollahi, Z.; Partovinia, A. Recent Advances on Pollutants Removal by Rice Husk as a Bio-Based Adsorbent: A Critical Review. *J. Environ. Manag.* **2019**, *246*, 314–323. [CrossRef]
21. Pak, H.; Phiri, J.; We, J.; Jung, K.; Oh, S. Adsorptive Removal of Arsenic and Lead by Stone Powder/Chitosan/Maghemite Composite Beads. *Int. J. Environ. Res. Public Health* **2021**, *18*, 8808. [CrossRef]
22. Sun, X.; Huang, H.; Zhao, D.; Lin, J.; Gao, P.; Yao, L. Adsorption of Pb^{2+} onto Freeze-Dried Microalgae and Environmental Risk Assessment. *J. Environ. Manag.* **2020**, *265*, 110472. [CrossRef]
23. Chen, S.; Zhu, M.; Guo, X.; Yang, B.; Zhuo, R. Coupling of Fenton Reaction and White Rot Fungi for the Degradation of Organic Pollutants. *Ecotoxicol. Environ. Saf.* **2023**, *254*, 114697. [CrossRef]
24. Gao, X.; Wei, M.; Zhang, X.; Xun, Y.; Duan, M.; Yang, Z.; Zhu, M.; Zhu, Y.; Zhuo, R. Copper Removal from Aqueous Solutions by White Rot Fungus Pleurotus Ostreatus GEMB-PO1 and Its Potential in Co-Remediation of Copper and Organic Pollutants. *Bioresour. Technol.* **2024**, *395*, 130337. [CrossRef]
25. Vale, M.A.; Ferreira, A.; Pires, J.C.M.; Gonçalves, G.A.L. CO_2 Capture Using Microalgae. In *Advances in Carbon Capture: Methods, Technologies and Applications*; Woodhead Publishing: Sawston, UK, 2020; pp. 381–405. [CrossRef]
26. Abdel-Raouf, N.; Al-Homaidan, A.A.; Ibraheem, I.B.M. Microalgae and Wastewater Treatment. *Saudi J. Biol. Sci.* **2012**, *19*, 257–275. [CrossRef]
27. Çelekli, A.; Bozkurt, H. Bio-Sorption of Cadmium and Nickel Ions Using Spirulina Platensis: Kinetic and Equilibrium Studies. *Desalination* **2011**, *275*, 141–147. [CrossRef]
28. Aksu, Z.; Dönmez, G. Binary Biosorption of Cadmium(II) and Nickel(II) onto Dried Chlorella Vulgaris: Co-Ion Effect on Mono-Component Isotherm Parameters. *Process Biochem.* **2006**, *41*, 860–868. [CrossRef]
29. Tien, C.J. Biosorption of Metal Ions by Freshwater Algae with Different Surface Characteristics. *Process Biochem.* **2002**, *38*, 605–613. [CrossRef]
30. Tüzün, I.; Bayramoğlu, G.; Yalçin, E.; Başaran, G.; Çelik, G.; Arica, M.Y. Equilibrium and Kinetic Studies on Biosorption of Hg(II), Cd(II) and Pb(II) Ions onto Microalgae Chlamydomonas Reinhardtii. *J. Environ. Manag.* **2005**, *77*, 85–92. [CrossRef]
31. Fraile, A.; Penche, S.; González, F.; Blázquez, M.L.; Muñoz, J.A.; Ballester, A. Biosorption of Copper, Zinc, Cadmium and Nickel by Chlorella Vulgaris. *Chem. Ecol.* **2005**, *21*, 61–75. [CrossRef]
32. Mehta, S.K.; Gaur, J.P. Removal of Ni and Cu from Single and Binary Metal Solutions by Free and Immobilized Chlorella Vulgaris. *Eur. J. Protistol.* **2001**, *37*, 261–271. [CrossRef]
33. Plöhn, M.; Escudero-Oñate, C.; Funk, C. Biosorption of Cd(II) by Nordic Microalgae: Tolerance, Kinetics and Equilibrium Studies. *Algal Res.* **2021**, *59*, 102471. [CrossRef]
34. Hockaday, J.; Harvey, A.; Velasquez-Orta, S. A Comparative Analysis of the Adsorption Kinetics of Cu^{2+} and Cd^{2+} by the Microalgae Chlorella Vulgaris and Scenedesmus Obliquus. *Algal Res.* **2022**, *64*, 102710. [CrossRef]
35. Bordoloi, N.; Goswami, R.; Kumar, M.; Kataki, R. Biosorption of Co (II) from Aqueous Solution Using Algal Biochar: Kinetics and Isotherm Studies. *Bioresour. Technol.* **2017**, *244*, 1465–1469. [CrossRef]
36. Skousen, J.G.; Sexstone, A.; Ziemkiewicz, P.F. Acid Mine Drainage Control and Treatment. In *Reclamation of Drastically Disturbed Lands*; American Society of Agronomy: Madison, WI, USA, 2015; pp. 131–168. [CrossRef]
37. Phiri, J.T. Biosorption of Cd2+, Co2+, and Cu2+ onto Chlorella Vulgaris, Scenedesmus sp., and Spirulina Platensis under Acidic and Neutral Conditions. Master's Thesis, School of Architectural, Civil, Environmental and Energy Engineering, Major in Civil Engineering The Graduate School, Kyungpook National University, Daegu, Republic of Korea, 2022.
38. Oh, S.; Kwak, M.Y.; Shin, W.S. Competitive Sorption of Lead and Cadmium onto Sediments. *Chem. Eng. J.* **2009**, *152*, 376–388. [CrossRef]
39. Dubinin, M.M. The Potential Theory of Adsorption of Gases and Vapors for Adsorbents with Energetically Nonuniform Surfaces. *Chem. Rev.* **1960**, *60*, 235–241. [CrossRef]
40. Gupta, V.K.; Rastogi, A. Equilibrium and Kinetic Modelling of Cadmium(II) Biosorption by Nonliving Algal Biomass Oedogonium Sp. from Aqueous Phase. *J. Hazard. Mater.* **2008**, *153*, 759–766. [CrossRef]
41. Kumar, M.; Singh, A.K.; Sikandar, M. Study of Sorption and Desorption of Cd (II) from Aqueous Solution Using Isolated Green Algae Chlorella Vulgaris. *Appl. Water Sci.* **2018**, *8*, 225. [CrossRef]
42. Gu, S.; Lan, C.Q. Biosorption of Heavy Metal Ions by Green Alga *Neochloris oleoabundans*: Effects of Metal Ion Properties and Cell Wall Structure. *J. Hazard Mater.* **2021**, *418*, 126336. [CrossRef]
43. Cruz-Lopes, L.P.; Macena, M.; Esteves, B.; Guiné, R.P.F. Ideal PH for the Adsorption of Metal Ions Cr^{6+}, Ni^{2+}, Pb^{2+} in Aqueous Solution with Different Adsorbent Materials. *Open Agric.* **2021**, *6*, 115–123. [CrossRef]
44. Driver, T.; Bajhaiya, A.K.; Allwood, J.W.; Goodacre, R.; Pittman, J.K.; Dean, A.P. Metabolic Responses of Eukaryotic Microalgae to Environmental Stress Limit the Ability of FT-IR Spectroscopy for Species Identification. *Algal Res.* **2015**, *11*, 148–155. [CrossRef]
45. Mecozzi, M.; Pietroletti, M.; Tornambé, A. Molecular and Structural Characteristics in Toxic Algae Cultures of *Ostreopsis ovata* and *Ostreopsis* spp. Evidenced by FTIR and FTNIR Spectroscopy. *Spectrochim. Acta A Mol. Biomol. Spectrosc.* **2011**, *78*, 1572–1580. [CrossRef]
46. Eren, E.; Afsin, B.; Onal, Y. Removal of Lead Ions by Acid Activated and Manganese Oxide-Coated Bentonite. *J. Hazard. Mater.* **2009**, *161*, 677–685. [CrossRef]

47. Chang, H.H.; Tung, H.H.; Chao, C.C.; Wang, G.S. Occurrence of Haloacetic Acids (HAAs) and Trihalomethanes (THMs) in Drinking Water of Taiwan. *Environ. Monit. Assess.* **2010**, *162*, 237–250. [CrossRef] [PubMed]
48. Dissolved Organic Carbon I DOC Analyzers & Sensors I Real Tech Water. Available online: https://realtechwater.com/parameters/dissolved-organic-carbon/ (accessed on 29 January 2023).